

$n + {}^6\text{Li}$ system investigated with the resonating-group method: Effects of channel coupling

Y. Fujiwara* and Y. C. Tang

School of Physics, University of Minnesota, Minneapolis, Minnesota 55455

(Received 17 February 1984)

Channel-coupling effects on the properties of the $n + {}^6\text{Li}$ system are studied. The channels included are $n + {}^6\text{Li}$, $n + {}^6\text{Li}^*$, and ${}^3\text{H} + \alpha$ channels. The calculation shows that there exist $S = \frac{1}{2}$, $L = 0$ and 1 resonance states in the $n + {}^6\text{Li}$ continuum, in agreement with the result of a recent R -matrix study. In addition, it is found that the ${}^3\text{H} + \alpha$ channel has a substantial influence, indicating that the energetically most-favored cluster configuration must always be considered in a resonating-group investigation. The coupling between $n + {}^6\text{Li}$ and $n + {}^6\text{Li}^*$ channels turns out generally to be fairly weak, although it does become somewhat enhanced when the ${}^3\text{H} + \alpha$ channel is included in the calculation.

I. INTRODUCTION

In a recent investigation,¹ hereafter referred to as FT1, we have studied the influence of the clustering and charge-form-factor behavior of ${}^6\text{Li}$ on the properties of the $n + {}^6\text{Li}$ system. By examining the $n + {}^6\text{Li}$ cross-section and phase-shift results obtained with a number of suitably chosen ${}^6\text{Li}$ internal functions, we came to the conclusion that (i) for a proper description of the resonance behavior of the $n + {}^6\text{Li}$ system in the low-energy region, the correlation property of ${}^6\text{Li}$ in terms of $d + \alpha$ clustering is of critical importance; and (ii) for a careful investigation of the $n + {}^6\text{Li}$ scattering behavior at high energies, one must adopt a ${}^6\text{Li}$ internal function which is flexible enough to yield correct charge-form-factor values over a wide range of q^2 .

In this investigation, we continue our study of the $n + {}^6\text{Li}$ system by examining the effect of channel coupling. To achieve this purpose, we perform a resonating-group calculation by taking $n + {}^6\text{Li}$, $n + {}^6\text{Li}^*$, and ${}^3\text{H} + \alpha$ channels into account, with ${}^6\text{Li}$ and ${}^6\text{Li}^*$ being $T = 0$ states described by translationally invariant $(1s)^4(1p)^2$ harmonic-oscillator shell-model functions representing $d + \alpha$ cluster configurations with relative orbital angular momenta I equal to 0 and 2, respectively. The information we seek can then be obtained by comparing the results from a single-channel calculation (SC), consisting of only the $n + {}^6\text{Li}$ channel, a coupled-channel calculation (CC), consisting of $n + {}^6\text{Li}$ plus $n + {}^6\text{Li}^*$ channels, and a full calculation (full), including all three channels.

A three-channel study with $n + {}^6\text{Li}$, $n + {}^6\text{Li}^*$, and ${}^3\text{H} + \alpha$ channels has recently been reported (Ref. 2, hereafter referred to as FT2). The emphasis there was, however, to examine channel-coupling effects of the $n + {}^6\text{Li}$ and $n + {}^6\text{Li}^*$ channels on the bound-state and phase-shift properties of the energetically most-favored ${}^3\text{H} + \alpha$ cluster configuration. In the present study, the discussion will instead be centered on the $n + {}^6\text{Li}$ channel as incident channel. Our hope is that, with this and previous^{1,2} studies, we can achieve a rather detailed understanding of the

level structure and reaction mechanisms in the seven-nucleon system.³

Experimental $n + {}^6\text{Li}$ scattering and reaction data have recently been summarized by Knox and Lane.⁴ In addition, these authors have performed a careful R -matrix analysis and obtained interesting information concerning the level structure of ${}^7\text{Li}$. As will be shown here, our results generally agree quite well with their analysis of the experimental data. However, some relatively minor differences do exist and these will be discussed below.

In Sec. II, a very brief discussion of the formulation is given. The results are presented in Sec. III, where channel-coupling effects in both $S = \frac{1}{2}$ and $\frac{3}{2}$ spin-angular-momentum states of the $n + {}^6\text{Li}$ system will be considered. In the case where $S = \frac{1}{2}$, we shall discuss the results from SC, CC, and full calculations. On the other hand, since the ${}^3\text{H} + \alpha$ channel has S equal to $\frac{1}{2}$, only the SC and CC results can be compared in $S = \frac{3}{2}$ states. Finally, in Sec. IV, we summarize the findings of this investigation and make some concluding remarks.

II. FORMULATION

The formulation of our present multichannel resonating-group calculation is very similar to that described in FT2; hence, only a brief discussion will be given here. As was mentioned in the Introduction, the internal functions of ${}^6\text{Li}$ and ${}^6\text{Li}^*$ will be taken as $(1s)^4(1p)^2$ harmonic-oscillator functions describing $d + \alpha$ cluster configurations with internal orbital angular momenta I equal to 0 and 2, respectively. The width parameter of this oscillator well is chosen to be 0.278 fm^{-2} , such that a correct result for the ${}^6\text{Li}$ rms charge radius is achieved.⁵ For the ${}^3\text{H}$ and α clusters, we similarly use wave functions which correspond to lowest configurations in harmonic-oscillator wells. The width parameters of these latter wells are assumed to be the same as that for the ${}^6\text{Li}$ and ${}^6\text{Li}^*$ clusters, in order to reduce substantially the computational effort.

The nucleon-nucleon potential adopted has a Serber ex-

change mixture (i.e., $u = 1$); it is the same as that used in FT1. For simplicity in calculation, we have again omitted the Coulomb contribution by letting the charge of the proton be infinitesimally small. This is certainly a reasonable simplification to make since, for the $n + {}^6\text{Li}$ channel which is of main interest here, the resultant omission of the exchange Coulomb interaction will have little significance.

With respect to the $n + {}^6\text{Li}$ channel, the calculated threshold energies for the $n + {}^6\text{Li}^*$ and ${}^3\text{H} + \alpha$ channels are 3.67 and -3.45 MeV, respectively. These are in reasonable agreement with the empirically determined values of 3.60 and -4.78 MeV.

The results from SC, CC, and full calculations will be compared through the phase shift $\delta_{L0,L0}^L$ and the reflection coefficient $\eta_{L0,L0}^L$ characterizing the diagonal element of the S matrix, and the transmission coefficients $\eta_{L,L0}^L$ and $\eta_{l2,L0}^L$ of the off-diagonal elements. As was similarly adopted in FT2, the indices of these S -matrix quantities have the following meaning. The superscript represents the total orbital angular momentum of the system. The subscripts on the right-hand side of the comma represent the (II) value ($I=0$) of the $n + {}^6\text{Li}$ incident channel, with l ($l=L$) being the relative orbital angular momentum between the neutron and the ${}^6\text{Li}$ cluster. As for the subscripts appearing on the left-hand side of the comma, a single digit denotes that the exit channel is the ${}^3\text{H} + \alpha$ channel with L being the relative orbital angular momentum between the ${}^3\text{H}$ and the α clusters, and a double digit (II) with $I=2$ denotes that the exit channel is the $n + {}^6\text{Li}^*$ channel with l representing now the relative orbital angular momentum between the neutron and the ${}^6\text{Li}^*$ cluster.

III. RESULTS

The results for the phase shift, the reflection coefficient, and the transmission coefficient in $S = \frac{1}{2}$ and $\frac{3}{2}$ states with $L=0-3$ are shown in Figs. 1–8 as a function of E , the relative energy of the neutron and the ${}^6\text{Li}$ cluster in the c.m. system. In these figures, the values obtained in the SC, CC, and full cases are represented by dashed curves, solid circles or dot-dashed curves, and solid curves, respectively. For clarity in presentation, we shall generally not show the transmission coefficient for transition into a weakly coupled state where its value is smaller than about 0.1 in the whole range of relative energy considered (i.e., 0–25 MeV).

A. $S = \frac{1}{2}$ states

(i) $L=0$ state (Fig. 1). The most notable features are that phase-shift values in SC and CC cases are nearly identical and the transmission coefficient $\eta_{22,00}^0$ in the CC calculation is quite small, especially in the low-energy region. This indicates that the direct coupling between $n + {}^6\text{Li}$ and $n + {}^6\text{Li}^*$ channels is very weak in the $L=0$ state. As a partial explanation of this, we note that the relative orbital angular momentum l is equal to 2 in the $n + {}^6\text{Li}^*$ channel and, hence, the coupling may be reduced because of centrifugal-barrier effects. Even so, however,

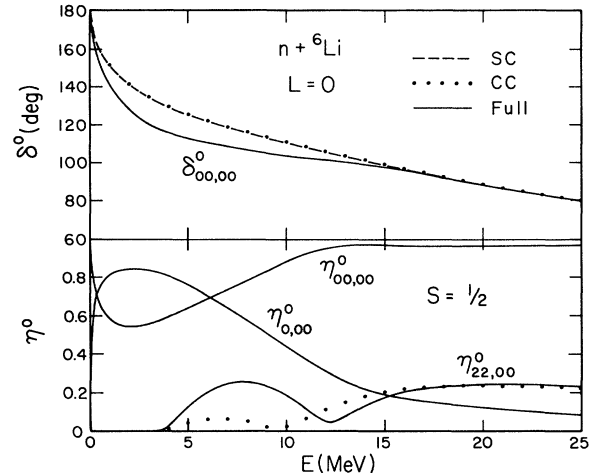


FIG. 1. Calculated $S = \frac{1}{2}$ phase shifts, reflection coefficient, and transmission coefficients for $L=0$ in the $n + {}^6\text{Li}$ channel. The dashed curve, solid circles, and solid curve represent results obtained with the SC, CC, and full calculations, respectively.

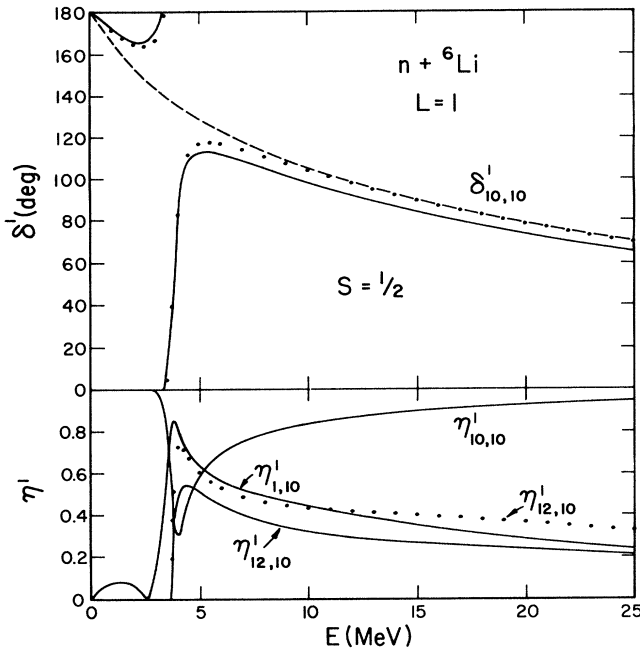
this is a rather surprising finding, in view of the fact that ${}^6\text{Li}$ and ${}^6\text{Li}^*$ are known to have similar intrinsic structures and belong to the same rotational band.

From Fig. 1, one further notes that there exists rather strong coupling between the $n + {}^6\text{Li}$ channel and the ${}^3\text{H} + \alpha$ channel. In fact, with the latter channel included, the coupling between $n + {}^6\text{Li}$ and $n + {}^6\text{Li}^*$ channels becomes even somewhat enhanced, as can be seen by the larger magnitude of $\eta_{22,00}^0$ in the full calculation (see also Ref. 6). This demonstrates, therefore, the important role played by the ${}^3\text{H} + \alpha$ channel and reminds one that, for a proper consideration of the properties of a nuclear system, the energetically most-favored cluster configuration must always be taken into account in the calculation.

With the full calculation, the phase-shift curve becomes quite flat in the energy region between about 5 and 10 MeV. This may indicate the presence of a very broad $\frac{1}{2}^+$ state in the $n + {}^6\text{Li}$ continuum, in qualitative agreement with the R -matrix result of Knox and Lane.⁴

Using the calculated values of the phase shift in the very low-energy region, we can compute the $n + {}^6\text{Li}$, $L=0$ scattering length. The resultant values are 2.60, 2.58, and 3.55 fm in the SC, CC, and full calculations, respectively. Comparing with the empirical value of 3.88 fm (Ref. 4), we note again that the inclusion of the ${}^3\text{H} + \alpha$ channel is important for a satisfactory explanation of the characteristics of the seven-nucleon system.

(ii) $L=1$ state (Fig. 2). In the SC case, there exists a bound state at -2.49 MeV and the phase-shift curve shows a smooth, monotonically decreasing behavior. With channel coupling taken into consideration, this state appears now in the lower-energy region, at -4.02 MeV in the CC case and -5.73 MeV in the full calculation. The large decrease in energy due to channel coupling is, of course, a strong demonstration of the well-known fact that the ground state of ${}^7\text{Li}$ does not have an $n + {}^6\text{Li}$ cluster structure. Additionally, one notes from Fig. 2 that the CC and full calculations exhibit clear evidence for the ex-

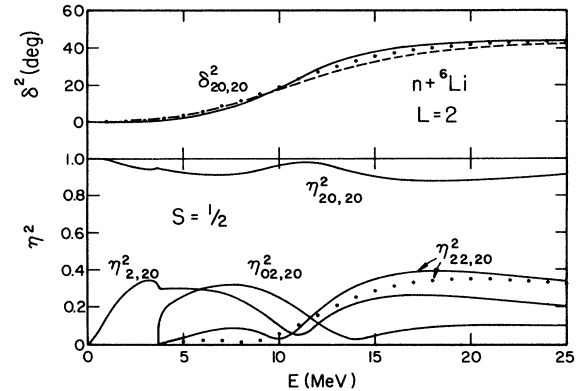
FIG. 2. Same as in Fig. 1, except that $L = 1$.

istence of a resonance state at about 0.2 MeV above the $n + {}^6\text{Li}^*$ threshold. This is interesting, since the R -matrix analysis of Ref. 4 also indicates the necessity of a broad $L = 1$, $S = \frac{1}{2}$ state in the $n + {}^6\text{Li}$ continuum. However, this latter analysis requires this state to have predominantly an $n + {}^6\text{Li}$ cluster configuration, although our finding shows that it has also an appreciable degree of $n + {}^6\text{Li}^*$ ($l = 1$) and ${}^3\text{H} + \alpha$ clustering, as evidenced by the large magnitudes of the transmission coefficients $\eta_{12,10}^1$ and $\eta_{1,10}^1$ in the resonance region.

Although the evidence for the existence of an $L = 1$ state is rather convincing, one should not rely upon the quantitative aspect of the calculated result. The adoption of a simple $(1s)^4(1p)^2$ configuration for ${}^6\text{Li}^*$ may have the consequence that this state appears with a relatively low excitation energy, quite close to the $n + {}^6\text{Li}^*$ threshold. If we had used a ${}^6\text{Li}^*$ wave function which adequately allows for a stronger degree of $d + \alpha$ clustering, our experience from FT1 indicates that the excitation energy would likely turn out to be larger by 2 or 3 MeV. Thus, it is reasonable to expect that this state may actually occur in the excitation region beyond 11 MeV, in which case it will be broad and hard to detect directly by experimental means.

The coupling between $n + {}^6\text{Li}$ and ${}^3\text{H} + \alpha$ channels is again rather strong. This is evidenced by the fact that, in the full calculation, the phase-shift curve deviates substantially from that in the CC case and that the transmission coefficient $\eta_{1,10}^1$ has an appreciable magnitude over a large energy range.

(iii) $L = 2$ state (Fig. 3). In this L state, both $n + {}^6\text{Li}^*$ and ${}^3\text{H} + \alpha$ channels have some influence on the $n + {}^6\text{Li}$ phase shift in the higher-energy region. At low energies less than about 10 MeV, however, it is seen from Fig. 3

FIG. 3. Same as in Fig. 1, except that $L = 2$.

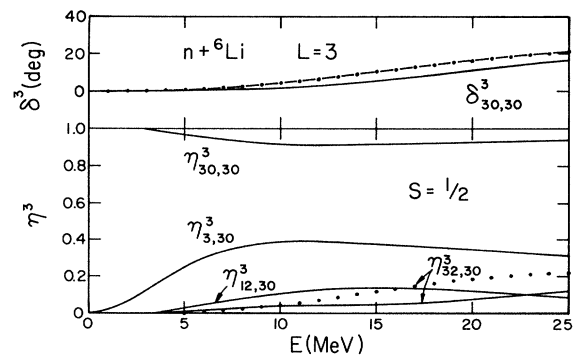
that the ${}^3\text{H} + \alpha$ channel seems to be more important.

In the full calculation it is noted that, at low energies, $\eta_{02,20}^2$ is appreciably larger than either $\eta_{22,20}^2$ or $\eta_{42,20}^2$. Thus, similar to the finding reported in FT2, we discover also here that the aligned configuration (i.e., $l = L - 2$) of the $n + {}^6\text{Li}^*$ channel is the most significant.

The transmission coefficient $\eta_{02,20}^2$ in the full calculation is substantially larger than that in the CC case (not shown in Fig. 3, for the reason stated above). This shows that there is again an enhancement in coupling between $n + {}^6\text{Li}$ and $n + {}^6\text{Li}^*$ channels due to the presence of the ${}^3\text{H} + \alpha$ configuration.

(iv) $L = 3$ state (Fig. 4). The similarity in the SC and CC phase-shift curves shows further that the direct coupling between $n + {}^6\text{Li}$ and $n + {}^6\text{Li}^*$ channels is weak. On the other hand, it is seen that the inclusion of the ${}^3\text{H} + \alpha$ channel in the full calculation does yield a significant change in the phase-shift result.

From the behavior of the transmission coefficients, one finds again that, at low energies, there is some evidence for the dominance of the aligned configuration of the $n + {}^6\text{Li}^*$ channel and for the above-mentioned feature of enhancement in coupling.

FIG. 4. Same as in Fig. 1, except that $L = 3$.

B. $S = \frac{3}{2}$ states

(i) $L=0$ state (Fig. 5). From Fig. 5, it is noted that the influence of the $n + {}^6\text{Li}^*$ channel on the $n + {}^6\text{Li}$ phase shift is larger than that in the corresponding $S = \frac{1}{2}$ state, and so is the transmission coefficient $\eta_{22,00}^0$. This shows that the coupling between $n + {}^6\text{Li}$ and $n + {}^6\text{Li}^*$ channels is somewhat stronger in the $S = \frac{3}{2}$ state than in the $S = \frac{1}{2}$ state. Even so, however, the effect of including the $n + {}^6\text{Li}^*$ channel is only moderate, as can be seen by the fairly small difference in phase-shift values obtained from the SC and CC calculations.

The calculated $n + {}^6\text{Li}$, $L=0$ scattering lengths are equal to 1.45 and 1.38 fm in the SC and CC cases, respectively, in reasonable agreement with the empirical value of 1.15 fm determined in Ref. 4. The finding that these two calculated values are not too different is another indication that the specific distortion effect of the $n + {}^6\text{Li}^*$ channel on the properties of the $n + {}^6\text{Li}$ system is not too large in the $L=0$ state.

The R -matrix analysis of Knox and Lane⁴ suggests the presence of a very broad $L=0$, $S = \frac{3}{2}$ state in the $n + {}^6\text{Li}$ continuum. Based on the behavior of the phase-shift curve in the CC calculation, we can neither support nor refute this claim, although the rather slow decrease of the calculated phase shift with energy may indicate that the existence of such a broad resonance state is not inconceivable.

(ii) $L=1$ state (Fig. 6). The distortion effect of the $n + {}^6\text{Li}^*$ channel on the $L=1$ resonance state is quite significant. With the $n + {}^6\text{Li}^*$ channel included, the resonance energy is lowered by about 1 MeV.

The transmission coefficient $\eta_{12,10}^1$ is larger than the transmission coefficient $\eta_{32,10}^1$ in the whole energy range considered. This is a demonstration of the fact that centrifugal-barrier effects are important in determining the degree of coupling between the $n + {}^6\text{Li}$ channel and different $n + {}^6\text{Li}^*$ configurations.

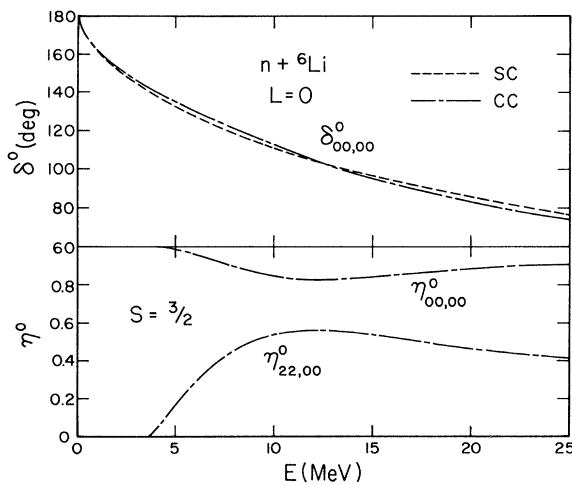


FIG. 5. Calculated $S = \frac{3}{2}$ phase shifts, reflection coefficient, and transmission coefficients for $L=0$ in the $n + {}^6\text{Li}$ channel. The dashed and dot-dashed curves represent results obtained with the SC and CC calculations, respectively.

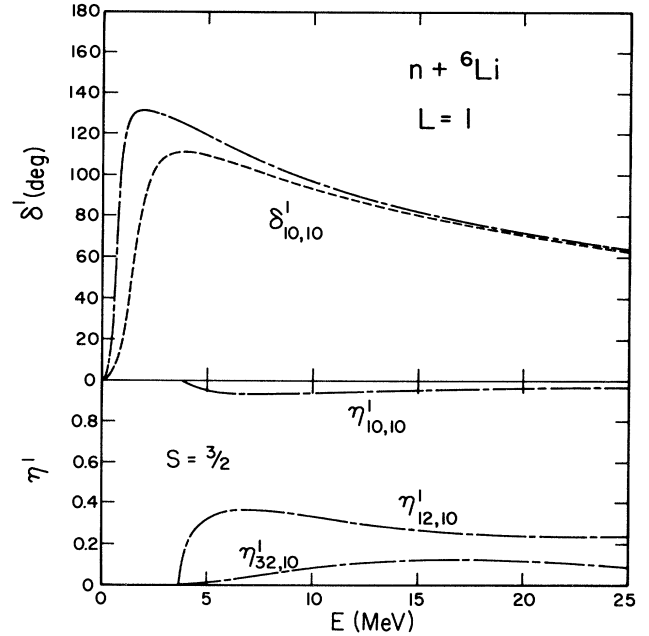


FIG. 6. Same as in Fig. 5, except that $L=1$.

(iii) $L=2$ state (Fig. 7). With the $n + {}^6\text{Li}^*$ channel taken into account, the $n + {}^6\text{Li}$ phase shift becomes larger in the whole energy range. At low energies, this increase is mainly effected by the coupling to the $n + {}^6\text{Li}^*$ aligned configuration, as can be seen by the larger magnitude of the transmission coefficient $\eta_{02,20}^2$. The situation is different at higher energies, where the $n + {}^6\text{Li}$ channel is now coupled more strongly to the $n + {}^6\text{Li}^*$, $l=2$ configuration. As has been explained in an analogous situation discussed in FT2, this can be understood as resulting from the presence of a very broad $l=2$ resonance with a $n + {}^6\text{Li}^*$ cluster configuration in the high-excitation region.

In the inset, we show the behavior around a phase-shift cusp. As is well understood,⁷ the appearance of such a cusp is the consequence of coupling between the $n + {}^6\text{Li}$ channel and the $l=0$ configuration of the $n + {}^6\text{Li}^*$ channel. In the present case, the cusp is not too prominent owing to the rather weak nature of the coupling.

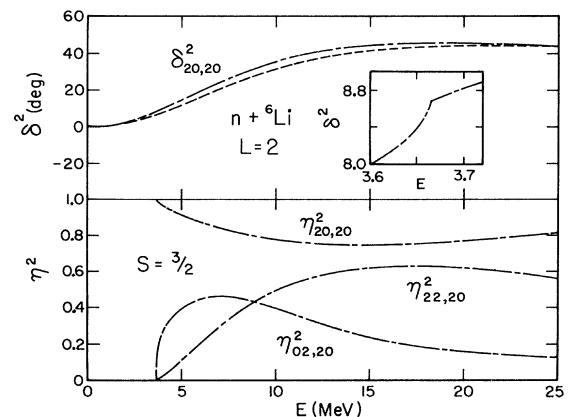


FIG. 7. Same as in Fig. 5, except that $L=2$.

(iv) $L=3$ (Fig. 8). The coupling is quite weak in this L state, as is evidenced by the near identity of the SC and CC phase-shift values and the small magnitude of the transmission coefficient $\eta_{12,30}^3$ for the dominant $n + {}^6\text{Li}^*$ aligned configuration.

C. Differential cross section

In Fig. 9, $n + {}^6\text{Li}$ differential cross sections in the SC, CC, and full cases are shown at 30 MeV. We choose to discuss at such a relatively high energy in order to make sure that sharp resonance levels do not dominate and that nucleon-exchange terms^{1,8} contribute in different angular regions.

It is seen from Fig. 9 that there is an appreciable, but not large, difference between the SC result on the one hand and the CC and full results on the other hand. This demonstrates that a proper consideration of channel-coupling effects is necessary for a detailed understanding of the properties of the $n + {}^6\text{Li}$ system. The cross-section results of the CC and full calculations turn out to be rather similar; this is understandable since, because of statistical weights, the cross-section behavior at this energy depends more heavily on contributions from $S = \frac{3}{2}$ states, for which the ${}^3\text{H} + \alpha$ channel plays no role in our calculation.

From Fig. 9, one further notes that the essential characteristics of the cross-section curve are, however, not modified by the addition of $n + {}^6\text{Li}^*$ and ${}^3\text{H} + \alpha$ channels. This is gratifying, since it means that the main features of nucleon-exchange contributions can already be semiquantitatively learned by performing a much simpler SC calculation.

IV. SUMMARY AND CONCLUSION

In summary, the main findings of this investigation are as follows:

(i) For a proper understanding of the level structure of the compound nucleus ${}^7\text{Li}$, one must take enough cluster configurations into account. In the $S = \frac{1}{2}$ state, our calculation with $n + {}^6\text{Li}$, $n + {}^6\text{Li}^*$, and ${}^3\text{H} + \alpha$ channels yields evidence for the existence of $L=0$ and 1 states in the $n + {}^6\text{Li}$ continuum, in agreement with the result from a recent R -matrix study.⁴ In the $S = \frac{3}{2}$ state, it is found that the inclusion of the $n + {}^6\text{Li}^*$ channel lowers the resonance energy of the $L=1$ state by a fairly large amount of about 1 MeV.

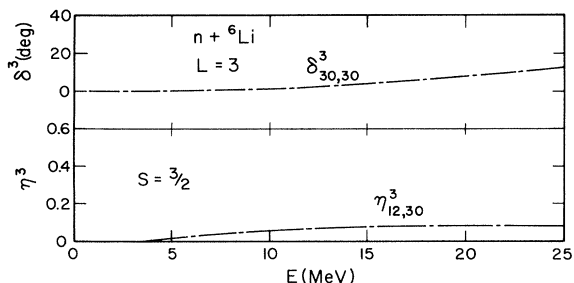


FIG. 8. Same as in Fig. 5, except that $L=3$.

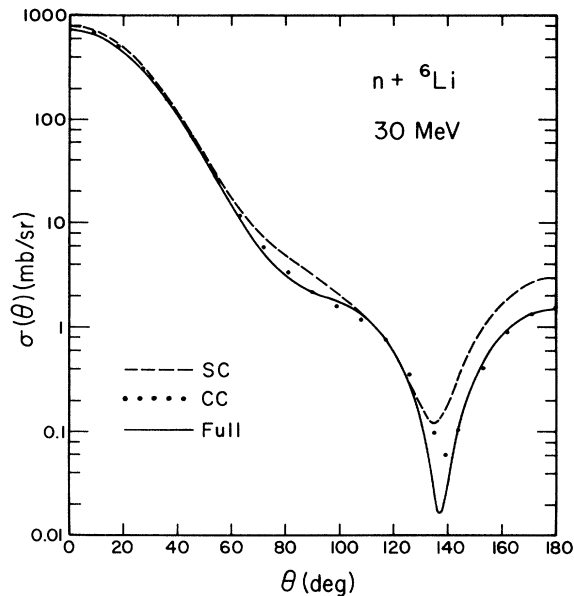


FIG. 9. Comparison of $n + {}^6\text{Li}$ differential cross sections at 30 MeV, obtained with the SC (dashed curve), CC (solid circles), and full (solid curve) calculations.

(ii) The phase-shift behavior of the $n + {}^6\text{Li}$ system is appreciably affected by the coupling to the ${}^3\text{H} + \alpha$ channel. This shows that, in a resonating-group study, the energetically most-favored cluster configuration must always be considered.

(iii) The coupling between $n + {}^6\text{Li}$ and $n + {}^6\text{Li}^*$ channels is not too strong. Its strength is somewhat smaller in the $S = \frac{1}{2}$ state than in the $S = \frac{3}{2}$ state. In the $S = \frac{1}{2}$ state, we find additionally that this coupling is generally enhanced when the ${}^3\text{H} + \alpha$ channel is included in the calculation.

(iv) Because of centrifugal-barrier effects, the aligned configuration of the $n + {}^6\text{Li}^*$ channel makes, in general, the most significant contribution.

In addition, we find that the essential characteristics of nucleon-exchange contributions in the $n + {}^6\text{Li}$ system is not much affected by the addition of $n + {}^6\text{Li}^*$ and ${}^3\text{H} + \alpha$ channels. Together with our previous finding reported in FT1 that these characteristics are also rather insensitive to the clustering and form-factor properties of ${}^6\text{Li}$, we can reasonably conclude that antisymmetrization effects may be qualitatively or even semiquantitatively understood by performing single-channel calculations utilizing simple internal wave functions for the incident and target clusters.

With the completion of this and previous^{1,2} investigations, we have learned that, for a detailed understanding of the properties of the seven-nucleon system, we must take into proper consideration target-clustering, form-factor, and channel-coupling effects. Therefore, the next logical step is to perform a multichannel study employing a realistic ${}^6\text{Li}$ wave function which accounts for the pres-

ence of a large degree of $d + \alpha$ clustering. This will certainly be a useful but very tedious task. However, we have recently developed the necessary mathematical technique⁹ which will enable us to complete such a calculation with reasonable computational effort. It is our hope that, with this planned study, we can eventually come to a rather complete understanding of the main characteristics of

the seven-nucleon system with respect to its level structure and reaction mechanisms.

This research was supported in part by the U.S. Department of Energy under Contract No. DOE/DE-AC02-79 ER 10364.

*Present address: Department of Physics, University of Michigan, Ann Arbor, MI 48109.

¹Y. Fujiwara and Y. C. Tang, Phys. Rev. C 27, 2457 (1983).

²Y. Fujiwara and Y. C. Tang, Phys. Rev. C 28, 1869 (1983).

³The seven-nucleon system has also been studied by other authors. The references are the following: M. V. Mihailović and M. Poljšak, Nucl. Phys. A311, 377 (1978); R. Beck, R. Krivec, and M. V. Mihailović, *ibid.* A363, 365 (1981); H. Kanada, T. Kaneko, and Y. C. Tang, *ibid.* A380, 87 (1982); H. M. Hofmann, T. Mertelmeier, and W. Zahn, *ibid.* A410, 208 (1983).

⁴H. D. Knox and R. O. Lane, Nucl. Phys. A403, 205 (1983).

⁵The ⁶Li wave function used here is the function ϕ_5 of FT1.

⁶Y. Fujiwara and Y. C. Tang, Phys. Lett. 131B, 261 (1983).

⁷E. P. Wigner, Phys. Rev. 73, 1002 (1948); L. D. Landau and E. M. Lifshitz, *Quantum Mechanics*, 3rd ed. (Pergamon, Oxford, 1977).

⁸D. Baye, J. Deenen, and Y. Salmon, Nucl. Phys. A289, 511 (1977); M. LeMere and Y. C. Tang, Phys. Rev. C 19, 391 (1979); M. LeMere, D. J. Stubeda, H. Horiuchi, and Y. C. Tang, Nucl. Phys. A320, 449 (1979); W. Sünkel and Y. C. Tang, *ibid.* A329, 10 (1979); K. Aoki and H. Horiuchi, Prog. Theor. Phys. 66, 1508 (1981); 66, 1903 (1981); 67, 1236 (1982); M. LeMere, Y. C. Tang, and H. Kanada, Phys. Rev. C 25, 2902 (1982); M. LeMere, Y. Fujiwara, Y. C. Tang, and Q. K. K. Liu, *ibid.* 26, 1847 (1982).

⁹Y. Fujiwara and Y. C. Tang, Nucl. Phys. A (to be published).